Twenty-Third Symposium (International) on Combustion/The Combustion Institute, 1990/pp. 707–713

A COMPUTATIONAL STUDY OF DIRECT SIMULATION OF HIGH SPEED MIXING LAYERS WITHOUT AND WITH CHEMICAL HEAT RELEASE

B. SEKAR
Vigyan Research Associates, Hampton, Va, USA.
AND
H. S. MUKUNDA
Indian Institute of Science, Bangalore, India.

This computational study is a direct simulation calculation of high speed reacting and non-reacting flows for H_2-air system. The Navier-stokes calculations are made for convective Mach numbers of 0.38 and 0.76 with hyperbolic tangent initial profiles and a single step reaction with fine grid distribution in a time accurate mode with higher order numerical methods till a statistical steady state is achieved. After this time, about 600 time sliced values of all the variables are stored for statistical analysis.

In this new study it is first shown that most of the problems of *high speed combustion* with *air* are characterised by *weak heat release*. The present calculations show that (i) the convective speed is reduced by heat release by 3–10% depending on convective Mach number, (ii) the variation of the mean and rms fluctuation of temperature can be explained on the basis of temperature fluctuation between the adiabatic flame temperature and the ambient, (iii) the growth rate with heat release is only 7% lower than without, (iv) the entrainment is 25% lower with heat release than without. These smaller differences in comparison to incompressible flow dynamics are argued to be due to larger enthalpy changes due to gas dynamics in comparison to heat release. *It is finally suggested that problems of reduced mixing at high speeds are not severely hampered by heat release.*

Introduction

Non-reacting and reacting incompressible mixing layers have been extensively explored both experimentally[1–3] and computationally.[4,5] Laboratory experiments have shown that the growth of the mixing layer is dominated by large scale quasi-two-dimensional vortices and their pairing in the early stages. The results of Hermanson and Dimotakis[2] also quoted in McMurtry et al.[4] for their experiments classified as 'weak heat release' cases with the peak to initial temperature ratio being 2.3 and 4 respectively show that heat release results in a slightly reduced growth of the shear layer (of the order of 10–15%). This result has been related to the reduction in turbulent shear stresses in the layer. Though the spacing of the cores of vortical structures have been shown not to be affected by heat release (p. 11, Ref. 4), it seems to have been accepted with reservation. McMurtry et al.[4] have conducted accurate temporal simulations of low Mach number flows without and with heat release. These have confirmed the experimental findings regarding the slower growth of the layer with heat release. Analysis seems to indicate the important role of thermal expansion and baroclinic torque terms in reducing the peak vorticity generation and enhancing diffusion. A spatial simulation of the incompressible mixing layer has been carried out by McInville et al.[5] The growth of the layer with distance shows an occasional decrease to an extent of 10%. This has been argued to be due to the phase relationships between the initial disturbance and the evolution of the roll up of the vortical structure downstream. Under suitable phase conditions the energy of the fluctuating part is drawn away into the mean flow thus decreasing the growth of the layer.

All the results noted above are for near incompressible flows. Supersonic mixing layers have been explored experimentally by Papamoschou and Roshko[6] who showed that the growth rate decreases with an increase in what is defined as the convective Mach number (M_c). M_c is the ratio of the difference in the velocities of the two streams to the sum of the acoustic speeds of the streams. The reduction in the growth rate is shown to be related to the reduced amplification of the distur-

bances in supersonic flows.[7] Lele[8] made direct simulation calculations of supersonic flows using higher order finite difference methods and validated the concept of M_c. Mukunda et al.[9] made similar calculations for non-reacting flows first establishing the results of Papamoschou and Roshko,[6] and then exploring the influence of initial profile (hyperbolic tangent and wake like profiles), the disturbance level and nature on the development of the mixing layer. All these studies are restricted to non-reacting flows. The present work aims at elucidating the effects of chemical heat release in high speed flows.

Some Considerations

The origins of the present problem lie in the recent interest in the development of the propulsion system for the national aerospace plane in USA. The typical flight Mach numbers go up to 21 and in the combustor up to 7. The combustor inlet temperatures are 1500–2500 K and pressures 0.05 to 0.15 MPa. At these conditions the reaction rates are very high and the steady combustion will be limited by mixing. The findings of reduced mixing in shear flows (i) due to high M_c,[6] and (ii) due to heat release in incompressible flows[2,3] have caused concern in the development of combustors for high speed flows and need for a basic examination of reacting high speed flows. The present contribution considers a typical case[10] of high speed mixing layer.

The fuel-oxidiser combination used in N_2 diluted H_2-air. In the present study the case with 10% (mass) H_2 in N_2 is treated in continuation with the earlier studies by Drummond and Mukunda.[10] The question of relevance of a study with a low fraction of hydrogen needs to be answered. One of the quantities of importance is the extent of heat release. In incompressible flows, one would obtain substantial variation in adiabatic flame temperature, T_{ad} (which is a good estimate of possible peak temperatures in the flame) with the hydrogen mass fraction (Y_{H_2}).The ratio $s(= T_{ad}/T_{in}$, where T_{in} is the initial temperature) for T_{in} = 300 K would be about 8 for pure H_2 and about 5 for Y_{H_2} = 0.1. One would want to examine if the behavior of 's' would be similar for the case of high speed applications. Computation of T_{ad} shows that with T_{in} = 2000 K, s = 1.5 for pure H_2 and 1.47 for Y_{H_2} = 0.1. Two important facts from these values are that (i) the T_{ad} is virtually the same for pure and diluted H_2, and (ii) the temperature ratio is not large. In fact, it is lower than the values used for the case of weak heat release in the experiments (see Ref 4). The reason why s is not different between Y_{H_2} = 1.0 and 0.1 is that most of the energy put in goes into the dissociation of the species including N_2 and the formation of energy absorbing NO. Though the present work treats essentially a single step reaction with N_2 as an inert, the use of a reversible reaction limits the peak temperature to s = 1.55, a value which is close to that from full chemistry.

The Computational Aspects

The problem is set into x-y cartesian coordinate system shown in Fig. 1. The entire calculation is made in dimensional form. The computational box ABCD has a length, x_m along x and y_m along y. It is divided into two sections at 0, $y = y_m/2$. The top section is the fuel region and the bottom, air. The initial profile is the hyperbolic tangent profile conventionally used in mixing layer studies given by $u_m = 1/2[(u_\infty + u_{-\infty}) + (u_\infty - u_{-\infty}) \tanh ky]$ with the constant k taken here as 1800 m^{-1}.

Table I shows the parameters relevant to the cases considered. The velocity of the air stream is lower than that of the fuel in case M_c = 0.38, but is much more in the case M_c = 0.76. The momentum ratios indicate that the momenta are balanced for M_c = 0.38 but greatly in favour of the air stream for M_c = 0.76 case. This causes the shear layer to remain roughly in alignment with the central axis in the first case but to bend over towards the fuel side in the second case. The boundary layer thickness (δ) based on 99% free stream velocity criterion is 2 mm. The momentum defect thickness (θ) is 1.54 mm. This implies that for the x grid length of 100 mm, one can cover about 64 θ. The Re_δ based on the average properties is 3500 to 12000 for the two cases. If the reference speed is the difference in speeds between the streams, then Re works out to 250 to 400. These values are considered low enough to obtain realistic results using the direct simulation approach with the current day computational aids. It is for this range of values that Lele[8] has made direct simulation computations.

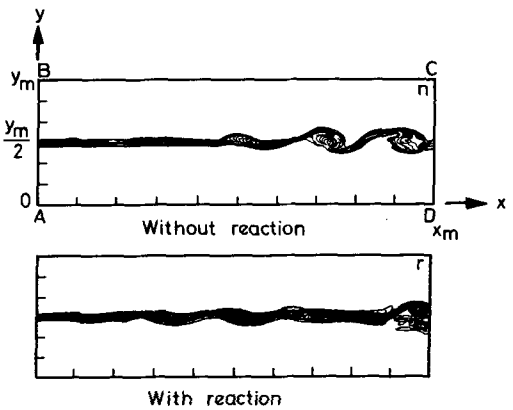

FIG. 1. The region of computation and the vorticity contour plots (n = no reaction, r = reaction).

TABLE I
Inflow parameters

composition	quantity	case 1	case 2
Fuel 0.1 H_2 + 0.9 N_2	ρ, kg/m^3	0.075	same
	u, m/s	2670.0	same
	M	2.0	same
	γ	1.3133	same
	sound speed, m/s	1336.0	same
	δ, mm	1.0	same
	μ, kg/m.s	5.5×10^{-5}	same
Oxidant 0.232 O_2 + 0.768 N_2	ρ, kg/m^3	0.175	0.175
	u, m/s	1814.0	4330.0
	M	2.1	5.25
	γ	1.296	same
	sound speed, m/s	864.3	same
	δ, mm	1.0	same
	μ, kg/m.s	6.2×10^{-5}	same
	u_c, m/s	2150.0	3670.0
	M_c	0.358	0.76

T = 2000 K, p = 0.101325 MPa, θ = 1.54 mm.

The disturbances are provided on the axial and lateral velocities (u_d and v_d) at $x = 0$. The disturbance is composed of a linear combination of several harmonic components of frequency determined from a spectral analysis of the flow field (at a downstream region) computed without any initial disturbances. The initial rms u fluctuation is about 3.68%. The boundary conditions on AD would be $u = u_m + u_d$, $v = v_d$, p = 0.101325 MPa, T = 2000 K and

$$Y_{H_2} = 0.1,\ Y_{O_2} = Y_{H_2O} = 0.0,\ Y_{N_2} = 0.9, \qquad (y_m > y > y_m/2)$$

$$Y_{O_2} = 0.232,\ Y_{H_2} = Y_{H_2O} = 0.0,\ Y_{N_2} = 0.768, \qquad (y_m/2 > y > 0)$$

At $x = x_m$ (on BC), first order extrapolation of the primitive variables is used. At $y = 0$ and y_m, the gradients ∂(property)/$\partial y = 0$ is set.

After detailed study[9] the region of calculation was chosen as 100 mm × 30 mm. In order to capture most scales of importance to grid distribution is chosen by considerations outlined in Ref. 9 and partly based on the discussion of Reynolds.[11] The number of grids used in the y direction is 101 or 151 for a region of 30 mm using stretched grid structure. The x direction (100 mm) is embedded with equispaced 201 or 251 grids of 0.5–0.4 mm in size. Calculations have been made to ensure grid independence of several details of the flow.[9]

The code used in the present calculations is the SPARK2D combustion code developed at the NASA LaRC over the past four years by Drummond and Carpenter (see Refs. 10 and 12). The code solves compressible Navier Stokes equation with species and energy conservation equations with conduction and diffusion models in the most general form.[10] Various algorithms can be adopted for integration of the differential equations. In the latest version,[12] it uses a 3rd order upwind biased algorithm for the streamwise direction based on the supersonic streamwise characteristics of the mixing layer. A 4th order central difference algorithm (Gottlieb) is used in the cross-stream direction. The temporal accuracy is second order. This choice represents a compromise between the accuracy of higher order numerical algorithms and the robustness and efficiency of lower order methods.

The reaction model chosen in $2H_2 + O_2 \rightleftharpoons 2H_2O$, and the reaction rate is given by

$$\dot{\omega}''' = A_f p^2 Y_{H_2}^2 Y_{O_2} e^{-E_f/RT} - A_b p Y_{H_2O}^2 e^{-E_b/RT} \qquad (1)$$

The backward rate constant in the above equation is chosen to be consistent with the equilibrium constant. The parameters of the forward rate constant are taken as $A_f = 1.1 \times 10^{19}$, and an activation energy, E_f = 67.2 kJ/mole. These values were obtained by requiring that the flame speed of the single step kinetics match with those from full chemistry. Limited comparison of Y_{H_2O} vs x at y = 0 in the mixing layer between single and multi-step kinetics is used to support the choice of the constants. It can be noticed that the reaction model

treats N_2 as an inert. The adiabatic flame temperature is obtained in this case as 3100 K and is realistic. The typical reaction time is about 10–50 μs and fluid flow time of 30–50 ms. These imply that the system is diffusion limited. The present calculations use a global unity Lewis number assumption for reference purposes.

In order to ensure that the flow attains a statistical steady state before sampling is performed, the code is run for each case for a duration of about three sweeps of the flow. Each sweep takes a time given by x_m/u_c and this is about 50 ms for M_c = 0.38 case and 30 ms for M_c = 0.76 case. The time step is typically 0.005 μs and it, therefore, takes 20000–30000 time steps before statistical steady state is achieved. After this, a total of about 600 time samples of all the flow field variables at specific x and y stations are stored at equal time intervals. These are subsequently analysed by a seperate statistical package. The results from this package include most quantities of turbulent flows. The shear layer thickness was obtained for u, Y_{H_2} and Y_{H_2O}. Of these, Y_{H_2O} alone tends to zero at $y \to \pm\infty$ and the others tend to nonzero finite values. In view of these features, the thicknesses are defined by

$$\delta_u = \frac{(u_\infty - u_{-\infty})}{(du_{\text{mean}}/dy)_{\max}} \tag{2}$$

with similar definition for Y_{H_2} and, $\delta_p = \int_{-\infty}^{\infty} Y_{H_2O} dy / Y_{H_2O_{\max}}$

The speed of vortical structures expected to be at the convective speed (u_c) is obtained by making instantaneous p vs x plots at some value of y near the center to cover the structure. These plots are made at a few times sufficiently spaced apart. The rate of movement of the point of peak pressure along x gives the convective speed. The convective speed is also calculated by using the formula,[6]

$$u_c = \frac{\sqrt{\rho_{-\infty}}\, u_{-\infty} + \sqrt{\rho_\infty}\, u_\infty}{\sqrt{\rho_{-\infty}} + \sqrt{\rho_\infty}} \tag{3}$$

Results and Discussion

While the calculations have been made for both the cases M_c = 0.38 and 0.76, the results presented here are largely for M_c = 0.38. The results for M_c = 0.76 will be brought out only where necessary. The non-reacting case will be called n and the reacting case as r.

Figure 2 shows that vorticity contour plot for both the cases n and r. While the rollup for the case n is very clear and occurs at x = 70 mm (45 θ), it appears that the contours are somewhat mixed up and the rollup is delayed to x = 95 mm for the case r (60 θ). Figure 2 has the plots of the mean velocity and temperature, and their rms fluctuations. The growth of the layer is shown by the dotted lines. One can notice the distinct change of growth rate with distance. Recognising that the first part of the growth is laminar, and the subsequent part transitional, similarity plots on the basis of the laminar and turbulent similarity coordinates have been established.[9]

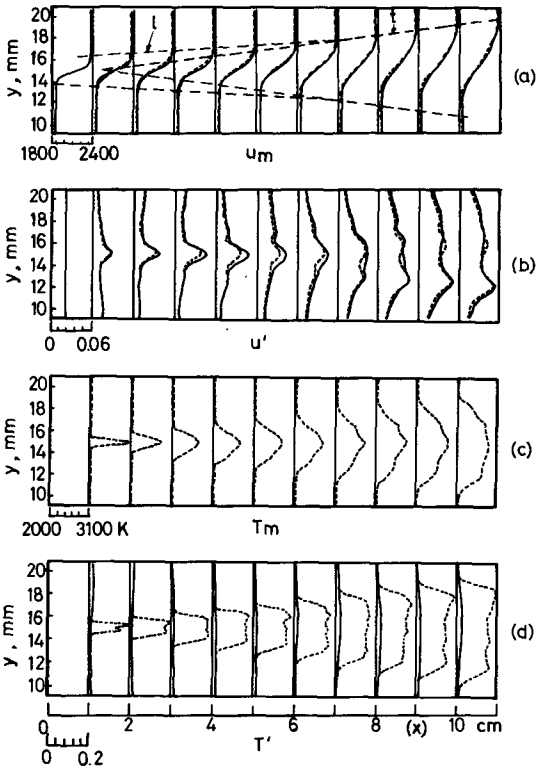

FIG. 2. The plots of u_m vs y (a), u' vs y (b), T_m vs y (c), T' (d) at various x stations.

The rms u fluctuations shown in Fig. 2b indicate that the maximum is about 6%. In the early development the fluctuations seem to have reduced peak. But later development does not seem to distinguish between the two cases n and r. The maximum of the mean peak static temperature of 3000 K as in Fig. 2c is close to T_{ad} from equilibrium thermochemistry. The reason for this is that the stagnation enthalpy is so large that with or without kinetic energy, the peak static temperature will remain about same through the adjustment of the extent of dissociation. The decrease of the mean peak temperature from 3000 K and to about 2650 K can be understood by an examination of the fluctuation history shown in Fig. 2d. The peak fluctuation goes to as high as 20% of the mean with the case r and

about 4% for the case n. The values seem fairly constant throughout the layer. It is the large fluctuation with chemistry that reduces the mean temperature along x. An examination of the temperature history at any x showed that it was essentially at either the peak temperature of 3100 K (the adiabatic flame temperature for stoichiometry) and the ambient of 2000 K with sharp transition. This picture is consistent with reaction being fast compared to flow times. Examination of the data showed that the fractional residence time (α) at 3100 K decayed from 0.7 to 0.6 in the downstream region. The mean temperature at any point is given in terms of the two temperatures, T_1 and T_0 by, $T_m = \alpha T_1 + (1 - \alpha)T_0$. The root mean square fluctuation of temperature (T') is given by $T' = \sqrt{\alpha(T_1 - T_m)^2 + (1 - \alpha)(T_m - T_0)^2/T_m}$.

For the reacting case, $T_1 = 3100$ K, $T_0 = 2000$ K, $\alpha = 0.7$, one gets $T_m = 2770$ K and $T' = 0.18$. For the same temperatures, but $\alpha = 0.6$, $T_m = 2660$ K and $T' = 0.21$. These are the peak values seen in the Fig. 2d, particularly in the downstream region. This model is consistent with the observation that mixing is centered around interfacial sheets which have vortical structures. By the same kind of arguments, for the nonreacting situation for which $T_1 = 1900$ K, $T_0 = 2000$ K, $\alpha = 0.6$, one obtains $T_m = 1940$ K and $T' = 0.027$. T_1 is taken as 1900 K because it is seen that in this case the local static temperature goes down to 1900 K due to gas dynamic expansion of the fluid locally. These results are also consistent with those seen in Fig. 2d where the non-reacting flow shows the peak T' to be about 0.03.

A plot of the instantaneous p vs x at a specific y station for $M_c = 0.38$ case is shown in Fig. 3a. Firstly, it can be noticed from this plot that the change in pressure is by no means insignificant. It changes from 0.07 to 0.14 MPa along x (as also along y through the shear layer). For the case of $M_c = 0.76$, (not shown in the figure) the pressure variation is between 0.045 to 0.17 MPa. These pressure variations are inevitably accompanied by shocks and expansions. The plots of p vs x with reaction also show similar changes in pressure, without any other qualitative difference. The local Mach number plot with x shown in Fig. 3b indicates that reaction reduces Mach number on an average. This is largely due to raise in acoustic speed due to increase in static temperature.

The instantaneous pressure plots, at different times are used to obtain the convective speeds as discussed earlier. The results for the two cases with and without reaction are shown in Table II. The convective speed obtained here seems to be higher than given by the formula by about 100 m/s at $M_c = 0.36$, but lower by 170 m/s at $M_c = 0.76$. In the former case, the p-x curves have the same shape at different times, the calculation is truely reflective

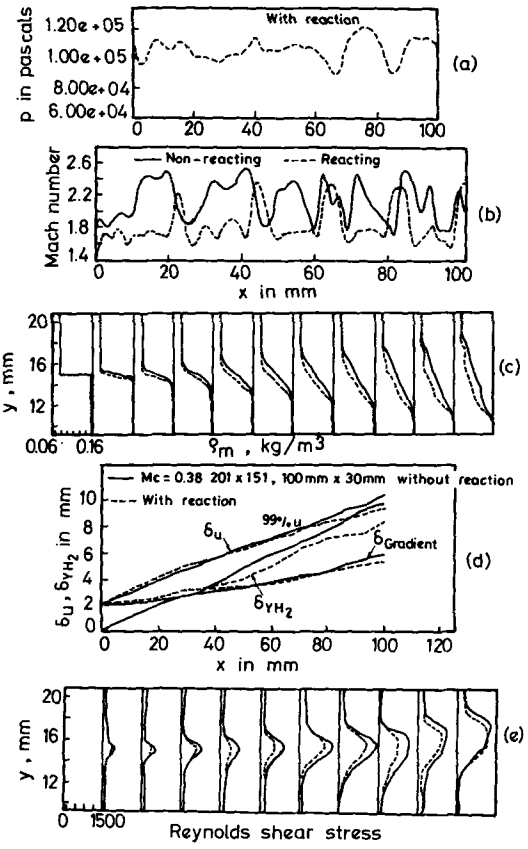

FIG. 3. The variation of static pressure with x ($y = y_m/2$) (a), Mach number with x ($y = y_m/2$) (b), ρ_m vs y at various x (c), δ_u, $\delta_{Y_{H_2}}$ thickness vs x (d), Reynolds stresses vs y at various x (e).

of a constant speed of the structure. At higher M_c, the p-x curves change their shape even with in the characteristic sweep time and there is a variation in the speed of the structures computed at different times. It may well be that the concept of convective speed cannot be directly used to characterise the flow because the structures undergo dilatation to a large extent. Reaction seems to reduce the convective speed of the structures substantially—a 8.5% (180 m/s) decrease at $M_c = 0.38$ and 3% decrease at $M_c = 0.76$. The effectiveness of heat release is lower at higher M_c. This is understandable because the static temperature changes due to gas dynamics become more and more comparable with the increase in temperature due to heat release. The fractional increase in the temperature at $M_c = 0.38$ is as much as 0.15 T_o and at $M_c = 0.76$, 0.25 T_o, whereas that due to combustion is 0.50 T_0. Thus as Mach number increases, changes due to gas dynamics become more relevent compared to those due to heat release. Figure 3c shows the variation

TABLE II
The convective speeds

M_c	u_c (no reaction) m/s	u_c (with reaction) m/s	u_c (formula) m/s
0.38	2260 ± 50	2083 ± 50	2150
0.76	3400 ± 150	3300 ± 100	3670

of density in the field. Firstly, it can be seen that the decrease in mean density is about 20% due to heat release. This decrease in density is composed of that due to temperature, pressure and hydrogen fraction. The changes in density contributed (i) by temperature is about 35%, (ii) by pressure about 20% at the maximum and (iii) by decrease in hydrogen fraction, about 10%. In comparison to case *n*, for the case *r*, temperature causes only decrease, pressure, either decrease or increase and hydrogen fraction always an increase in density. In the experiments and analysis conducted[2–5] on low Mach number flows with reaction the free stream density of the two fluids is not significantly different and the local temperature rise is significantly large compared to the ambient stream temperature. In these cases, the fractional change in density goes up to 0.4. In the present case, it is about 0.25 at the maximum. Several conclusions which follow from low Mach number reacting flow studies become weakly relevent at high speed consequent upon the above features (discussed below). The plots of hydrogen and water mass fraction show that their extent of growth follows that of velocity or temperature. This is due to unity Lewis number assumption made in the present work. Some aspects of the distribution of H_2 and H_2O will be different if a realistic trace diffusion model is adopted. The distribution of the H_2O and its rms fluctuation are close to that of temperature for the same reason that Lewis number is unity (hence both are not displayed here).

Figure 3d shows the plot of the thickness of the mixing layer based on u (δ_u) and Y_{H_2} ($\delta_{Y_{H_2}}$). The growth of δ_u measured by 99% criterion is around 8 mm in 100 mm. The growth measured by vorticity thickness is about 45% of δ_u. These are similar to those observed in subsonic flows.[2] The mass fraction profile grows from zero thickness and begins to acquire the profile similar to that of u early and displays an effective higher growth of 10 mm in 100 mm. The heat release seems to decrease the growth rate marginally. The u growth indicates about 7% decrease and Y_{H_2} growth shows a decrease of 10%. The growth in the early stages is uneven and has occasional low growth regions. These are due to coupling of the downstream region with initial disturbance pattern discussed earlier and also found in earlier work.[5] Figure 3e shows the plot of Reynolds shear stress in the field. The Reynolds stresses with heat release are generally smaller than those without heat release and contribution towards this comes from reduction in density. As the flow proceeds the differences seem to be decreasing. The decrease in the Reynolds stresses in the flow field due to heat release is argued to be the cause of reduced growth of the shear layer whose variation with axial distance is presented in Fig. 3d.

In addition to the above, the time and space spectra of u fluctuations, kinetic energy of fluctuations, vorticity distribution were examined without and with heat release. The kinetic energy of fluctuations showed at 10% decrease with the heat release, time and space spectra showed no discernable trends and vorticity distribution, a marginal change.

It is appropriate now to discuss the present results in the light of earlier work. There are no experimental studies in supersonic reacting flows for comparison. However, there are many studies in incompressible flows referred to earlier. The principal conclusions of the work of Refs. 2–4, are that the growth rate of the shear layer decreases with the extent of heat release. A careful examination of the data indicates that the scatter in the data is not small though it may not invalidate the result that the layer thickness decreases with heat release. While most of their discussion centres around the growth variation with decrease in density due to heat release, the growth rate variation with increase in the peak temperature is plotted. It is argued that the decrease in density causes dilatation and one would have to expect increase in growth rate. That the observed growth rate decreases—up to 10% in the incompressible case and to slightly lower extent in the present case at the same peak increment in temperature—is taken to indicate decrease in entrainment of the fluid, to a larger extent (20–25%). In the present case, the overall decrease in entrainment is estimated from the mass flux profiles to be 18% (M_c = 0.38) and 15% (M_c = 0.76). The decreasing influence of heat release in altering the dynamics of the flow is essentially due to the importance of enthalpy changes in the flow even without heat release. The vortex core spacing in the case of non-reacting flow is about three times the layer thickness. This should be compared with values of

about 1.5 in incompressible flows and 2–3 in high speed flows.[6] The enhanced core spacing in high speed flows is argued to be due to decreased rate of amplification of disturbances. The decreased rate causes the process of roll up to occur a slower rate. Heat release causes a slight reduction in the vortex spacing (to about 2.5 δ) and causes the distinction between the vortical structures to be less clear (see Fig. 1). Both these features have been discussed in incompressible flows.[2]

In summary, high speed reacting mixing layers are characterised by a 'weak heat release' situation along with gas dynamics playing a substantially larger role in affecting the growth of the layer compared to incompressible flows. Specifically,

(1) The significant role of heat release is to reduce the growth rate of the mixing layer by about 5–7% and reducing the convective speed of the structures by about 3–10% depending on the convective Mach number. Increased convective Mach number reduces the effect of heat release.

(2) The density changes in the flow are dominated by composition, pressure and temperature compared to the cases studied in incompressible flows in which temperature alone is the dominating factor. The reduction of entrainment in high speed flows due to density changes is much less than in incompressible flows.

(3) Many phenomena like reduction in Reynolds stresses, kinetic energy of fluctuations due to heat release are akin to those in incompressible flows, but to much less extent.

In view of the weaker role of heat release in affecting the dynamics of mixing layers in high speed flows, it is important to conclude that it is useful to concentrate on non-reacting flows for the mixing related issues like enhanced mixing concepts. The heat release mechanisms are likely to provide only a small perturbation and need not be a matter of major concern.

REFERENCES

1. Brown, G. L. and Roshko, A., J.: Fl. Mech. 91, 319 (1974).
2. Hermanson, J. C. and Dimotakis, P. E.: J. Fl. Mech. 199, 333 (1989).
3. Dimotakis, P. E.: 27th Aerospace Sciences meeting, AIAA 89-0269, (1989), Reno, Nevada.
4. McMurtry, P. A., Riley, J. J. and Metcalfe, R. W.: J. Fl. Mech. 199, 297 (1989).
5. McInville, R. M., Gatski, T. B. and Hassan, H. A.: AIAA J 23, 1165 (1985).
6. Papamoschou, D. and Roshko, A.: J. Fl. Mech. 197, 453; also see Papamoschou, D. AIAA Paper 89-0126, 27th Aerospace Sciences meeting, (1989), Reno, Nevada.
7. Sandham, N. and Reynolds, W.: 27th Aerospace Sciences meeting, AIAA 89-0371, (1989).
8. Lele, S. K.: 27th Aerospace Sciences meeting, AIAA-89-0374, (1989).
9. Mukunda, H. S., Sekar, B., Carpenter, M., Drummond, J. P. and Kumar, A.: Studies in the direct numerical simulation of high speed mixing layers, NASA TP (1989), to be released.
10. Drummond, J. P. and Mukunda, H. S.: Mixing enhancement in two-dimensional shear layers, NASA TM 1033, (1988).
11. Reynolds, W. C.: Whither turbulence conference, Cornell Uni., March (1989).
12. Carpenter, M. H.: A comparative study of high order and compact numerical algorithms with existing central and upwind algorithms, NASA CR (1989), to be released.